

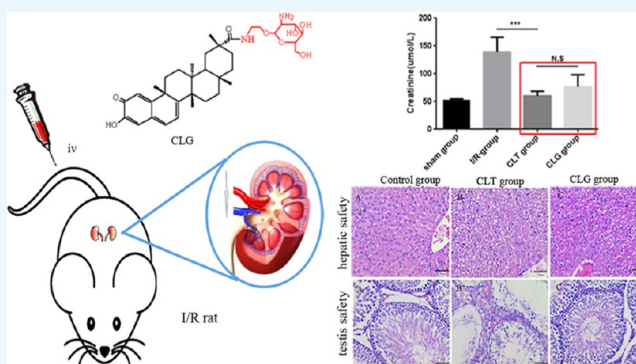
Novel Low-Toxic Derivative of Celastrol Maintains Protective Effect against Acute Renal Injury

Xun Hu, Mengdi Jia, Yu Fu, Pei Zhang, Zhirong Zhang,^{1b} and Qing Lin*^{1b}

Key Laboratory of Drug Targeting and Drug Delivery Systems, Ministry of Education, Department of Pharmaceutics, West China School of Pharmacy, Sichuan University, No. 17 People's South Road, Chengdu 610041, P. R. China

Supporting Information

ABSTRACT: This study aimed to novelly design and synthesize an amide derivative as a potential substitute of celastrol (CLT). We constituted the compound celastrol–glucosamine (CLG) by conjugating 1-(2-aminoethoxy)-2-glucosamine to celastrol (CLT) and confirmed its chemical structure by ¹H NMR, ¹³C NMR, and LC-MS/MS. Then, the potential efficacy of the CLG was investigated on renal ischemia–reperfusion injury animal models. The results demonstrated that the decorated compound CLG could completely reverse the disease progression as same as CLT. Furthermore, the toxicity of CLG was also fully evaluated in rat blood, liver, kidney, heart, spleen, lung, and reproductive system. Compared to the performance of CLT on normal organs, CLG could remarkably maintain high safety and significantly reduce the side effects. Taken together, the CLG could keep the same efficacy as CLT while processing lower toxicity in vivo.



1. INTRODUCTION

Renal disease is gradually rising around the world, which is a severe problem. It is reported that 6.5–10% population in developing country is suffering from kidney disease. Even worse, the incidence of kidney disease is reported to be 10.2–11.3% in China.¹ Furthermore, acute renal failure plays an important role in kidney disease. In that case, renal injury, which often occurs in various clinical therapy, such as kidney transplantation,² cardiac failure,³ kidney vascular surgery,⁴ and shock resuscitation,⁵ induced by ischemia–reperfusion (I/R) is the main reason of acute renal failure. This has been regarded as a serious health problem in present society.⁶ A variety of drugs have been identified including propofol,⁷ erythropoietin,⁸ and glutamine⁹ for treating renal I/R injury. However, the efficacy of these pharmaceuticals for IR-induced renal injury is still limited and these drugs are hard to translate into clinical application.¹⁰ Therefore, there is an urgent need for developing novel drugs for acute IR-induced renal injury.

Therefore, we attempted to obtain an effective but low-toxicity drug to ameliorate the current conditions. In the current study, we chose to construct an effective derivative through conjugating glucosamine to celastrol (CLT), also known as tripterine, which was the major biologically active component extracted from the traditional Chinese medicinal herb, *Tripterygium wilfordii* Hook (also known as Thunder of God Vine).¹¹

In previous studies, some research groups had successfully proved that CLT had diverse biological activities as an inhibitor of lipid peroxidation¹² and a downregulation mediator of anti-

inflammatory responses, such as interleukin-1 α ,¹³ tumor necrosis factor- α ,¹⁴ and nuclear factor κ B.¹⁵ Besides, CLT could also induce the heat shock response,¹⁶ increase the expression of cytoplasmic chaperones, and activate unfolded protein response.¹⁷ Specially, because of the anti-inflammatory and antioxidative activity, CLT was a potent agent for treating inflammatory disorders, such as arthritis,¹⁸ atherosclerosis,¹⁹ allergic asthma,²⁰ and Parkinson's disease.²¹ Recently, it was proven that CLT could protect cerebral ischemic injury and reduce brain infarct volume as well as water content in a rat stroke model.²² Furthermore, it also demonstrated that CLT was able to cure acute kidney disease, which was verified in protecting kidney I/R-induced injury.¹⁰ However, the long-term administration of CLT was always accompanied by systemic toxicities and multiple adverse effects, such as blood toxicity, hepatic damage, and reproductive disorder.²³ Given those conditions, we focused on the development of an alternative of CLT, seeking an identically efficient but a much safer derivative.

In the current study, we developed an amide derivative—celastrol–glucosamine (CLG) conjugate—and investigated the pharmacological properties mainly in efficacy and toxicity. The results suggested that the CLG could be used in acute kidney disease and really kept enough safety in organs and blood.

Received: November 30, 2017

Accepted: February 22, 2018

Published: March 6, 2018

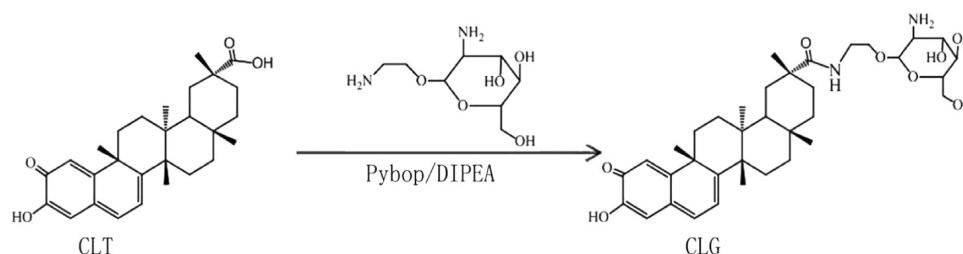


Figure 1. Synthesis of celastrol–glucosamine (CLG) conjugate. Reagents and conditions: dimethylformamide (DMF), room temperature (RT), 48 h.

2. RESULTS AND DISCUSSION

In the current study, we synthesized a new celastrol–glucosamine (CLG) conjugate, and, further, we verified that CLG could maintain the efficacy as CLT and significantly decrease the adverse effects on blood cells, liver, and testis. These results in rats suggested that the CLG may have the opportunity to be further developed in clinical trials.

2.1. Successful Synthesis and Characterization of CLG.

CLG was constructed as designed (Figure 1). The structure of CLG was confirmed by high-performance liquid chromatography–mass spectrometry (LC–MS) and (^1H NMR and ^{13}C NMR). Yield was 20%. ^1H NMR (400 MHz, CD_3OD): δ 7.26 (m, 1H), δ 6.71 (d, 1H), δ 6.44 (dd, 1H), δ 5.67 (M, 1H), δ 3.81–3.64 (m, 3H), δ 3.29 (m, 10H), δ 2.71 (m, 3H), δ 2.18–2.03 (m, 8H), δ 1.68 (m, 10H), ^{13}C NMR (151 MHz, CD_3OD): δ 182.96, 173.76, 168.32, 151.54, 139.66, 131.84, 125.09, 123.03, 122.56, 105.10, 82.22, 79.59, 75.07, 72.52, 65.71, 62.59, 61.52, 49.65, 49.01, 47.21, 46.37, 45.01, 44.27, 43.95, 42.89, 41.25, 39.92, 38.33, 36.59, 35.71, 35.35, 34.24, 33.69, 33.31, 26.56, 22.93, 15.25. ESI–MS: m/z [M + H] $^+$: 655.5 (Figures S1–S3).

Stability study showed that no released CLT was found in phosphate-buffered saline (PBS) at 37 °C for 24 h, which demonstrated that this type of conjugate was highly stable (Figure 2).

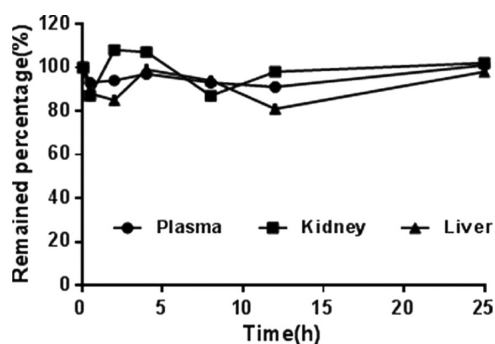


Figure 2. In vitro stability of CLG in biological samples. CLG was incubated with rat plasma, liver, or kidney homogenate for 24 h. All of the mixtures were incubated at 37 ± 1 °C in the shaking bath, and the samples were taken at the predetermined time points. Data represent mean \pm standard deviation (SD) ($n = 3$).

2.2. Maintaining Protective Effects of CLG against Renal I/R Injury in Rats as CLT. To investigate the protective effect of CLG on renal dysfunction caused by I/R injury, plasma creatinine (Cr) and blood urea nitrogen (BUN) levels at 24 h after renal reperfusion were measured (Figure 3A). Male SD rats (body weight of 200 ± 10 g) were randomly assigned into four groups ($n = 5$): sham-operated group, I/R

group, I/R + CLT group, and I/R + CLG group. In this experiment, the rats pretreated by CLG exhibited a significant decrease in concentration of BUN and Cr in a dose-dependent manner, similar to the rats pretreated with CLT (Figure 3A), compared with the sham group.

Then, the kidney was collected at 24 h after renal reperfusion with hematoxylin–eosin (H&E) staining and tested for renal damage score. The results suggested that there was no histological change in the sham-operated group (Figure 3B). But for the I/R group (Figure 3B), the obvious renal damage appeared, which was especially expressed in features of severe acute tubular damage, including tubular cell swelling, tubular dilatation, loss of brush border, and cellular infiltration. The symptomatic changes were distributed in the whole kidney cortex. Compared with the I/R group, these histological alterations were significantly attenuated in rats pretreated with CLT and CLG (Figure 3B), although dilatation of tubular lumen and degeneration of the renal tubular epithelial cells could still be found. In brief, the score of renal damage in the I/R group was much higher than that in the sham-operated group and the drug-given groups.

Apoptosis of renal cells in situ was assessed by terminal deoxynucleotidyl transferase biotin-dUTP nick end labeling (TUNEL) staining (Figure 3C). Only few apoptosis could be detected in the sham-operated group, with the AI (apoptotic index) of $15.25 \pm 1.73\%$. However, there was significantly increased apoptotic cells in the I/R group (Figure 3C), with the AI of $22.64 \pm 0.62\%$. In contrast, evident decline in the number of apoptotic cells was observed in the I/R group pretreated by CLG (Figure 3C) with the AI of $16.41 \pm 1.18\%$, similar to the I/R group pretreated by CLT (Figure 3C) with the AI of $17.94 \pm 0.63\%$.

According to the reported studies, the numbers of proinflammatory mediators, such as intercellular adhesion molecule-1 (ICAM-1) and inducible nitric oxide synthase (iNOS), would be elevated to a high level in the ischemic organ diseases,²⁴ suggesting that the severity of renal damage and dysfunction was positively associated with proinflammatory mediator levels.²⁵ Besides, CLT was quite effective to handle these problems.¹⁰ Therefore, in the experiment, we detected those proinflammatory mediators, including ICAM-1 and iNOS, that always amplified the inflammatory response and deteriorated tissue damage in morphology and function.²⁶ ICAM-1 was mainly detected in the damaged tubular cells by immunohistochemistry (Figure 3D). The expression of ICAM-1 in the kidney tissues significantly increased in the I/R group compared with those in the sham group, whereas the CLT and CLG could markedly inhibit the expression of ICAM-1 induced by I/R injury. In addition, the expression of iNOS appeared to be significantly increased in the kidneys, mainly located in the renal tubular cells (Figure 3E). Similarly, the

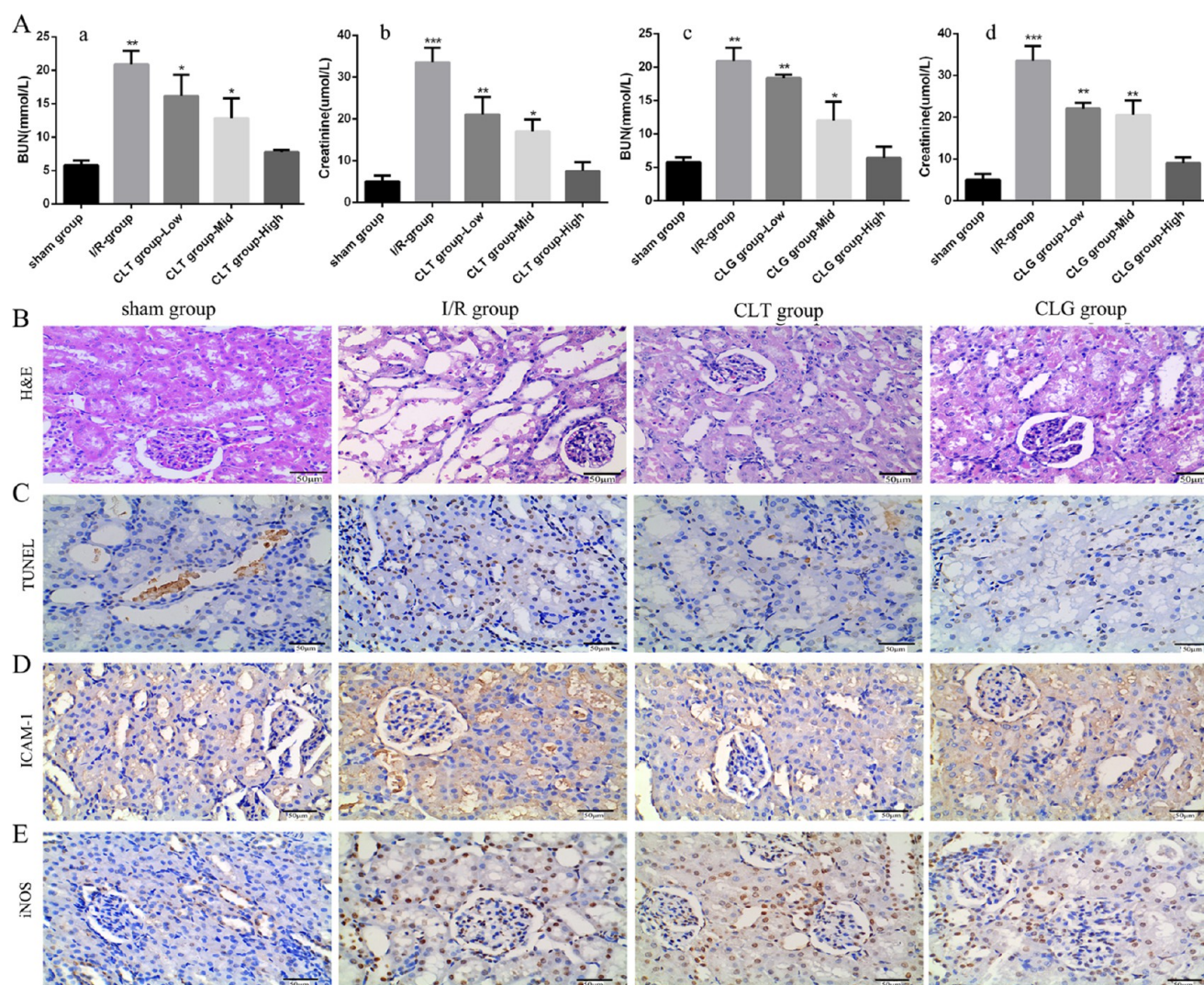


Figure 3. Therapeutic effect of CLT and CLG on the renal function in the I/R rats. (A) The plasma levels of BUN (A-a, A-c) and Cr (A-b, A-d) were measured in rats that were pretreated with CLT (the dosage ranged from 0.45 to 1.8 mg/kg) and CLG (the dosage ranged from 0.65 to 2.62 mg/kg) (all groups vs sham group, $n = 5$, mean \pm SD, $***p < 0.001$). (B) The respective light photomicrographs of hematoxylin–eosin (H&E)-stained renal tissue in rats pretreated with 0.45 mg/kg of CLT and 0.65 mg/kg of CLG [the sham group marked by (–); the I/R group marked by (+++); the CLT group marked by (+); and the CLG group marked by (+)]. (C) Representative light photomicrographs of TUNEL-stained kidney tissue. (D, E) The effect of CLT and CLG on inducible nitric oxide synthase (iNOS) and intercellular adhesion molecule-1 (ICAM-1) during renal I/R was detected by immunohistochemical analysis. Original magnification in all of the figures was 400 \times . All of the results are means of measurements from five replicates. [(–) represented normal; (+) minimal damage (less than 5% area of the cortex or outer medulla); (++) mild damage (5–25% area of the cortex or outer medulla); (+++) moderate damage (25–75% involvement of the cortex or outer medulla); (++++ severe damage (more than 75% involvement of the cortex or outer medulla)].

pretreatment of CLT and CLG also blocked the increase in the iNOS level. The results demonstrated that CLG could suppress the expression of ICAM-1 and iNOS as same as CLT did.

Taken together, all of those results implied that celastrol–glucosamine (CLG) conjugate could alleviate the renal damage and decrease the proinflammatory mediator caused by I/R injury as effectively as CLT.

2.3. CLG Reduced Adverse Effects in Blood System.

Previous studies suggested that rats treated with CLT would suffer developmental disorder of testicular atrophy, toxicity of blood system, and damage of liver.²³ Hence, we decided to compare the adverse effects of CLT and CLG on rats for a long period.

To investigate the toxicity differences between CLT and CLG in the blood system, both of them were injected into normal rats in the condition of dose gradient. Rats were

randomly divided into seven groups of five animals each. A control group; and in regard to CLT and CLG group, we set up a serial of dose gradient, in which the dose of CLT was 1.8, 0.9, and 0.45 mg/kg, equaling the dose of CLG of 2.62, 1.31, and 0.65 mg/kg. Then, we measured several blood routine indexes for 3 weeks, and it exhibited that CLT drastically affected the number of blood cells, but CLG had little influence on their number. In the results, white blood cells (WBCs) were quite susceptible to the dose change in CLT but not sensitive to the dose fluctuation of CLG (Figure 4A). Additionally, the number of lymphocytes (Figure 4B) and neutrophils (Figure 4C) similarly ranked to a high level after 3 week injection with CLT, which proved that CLT indeed led blood system to a defensive behavior with a dose-dependent tendency.

Except for influencing WBC in the blood system, red blood cells (RBCs) were also profoundly impacted by CLT (Figure

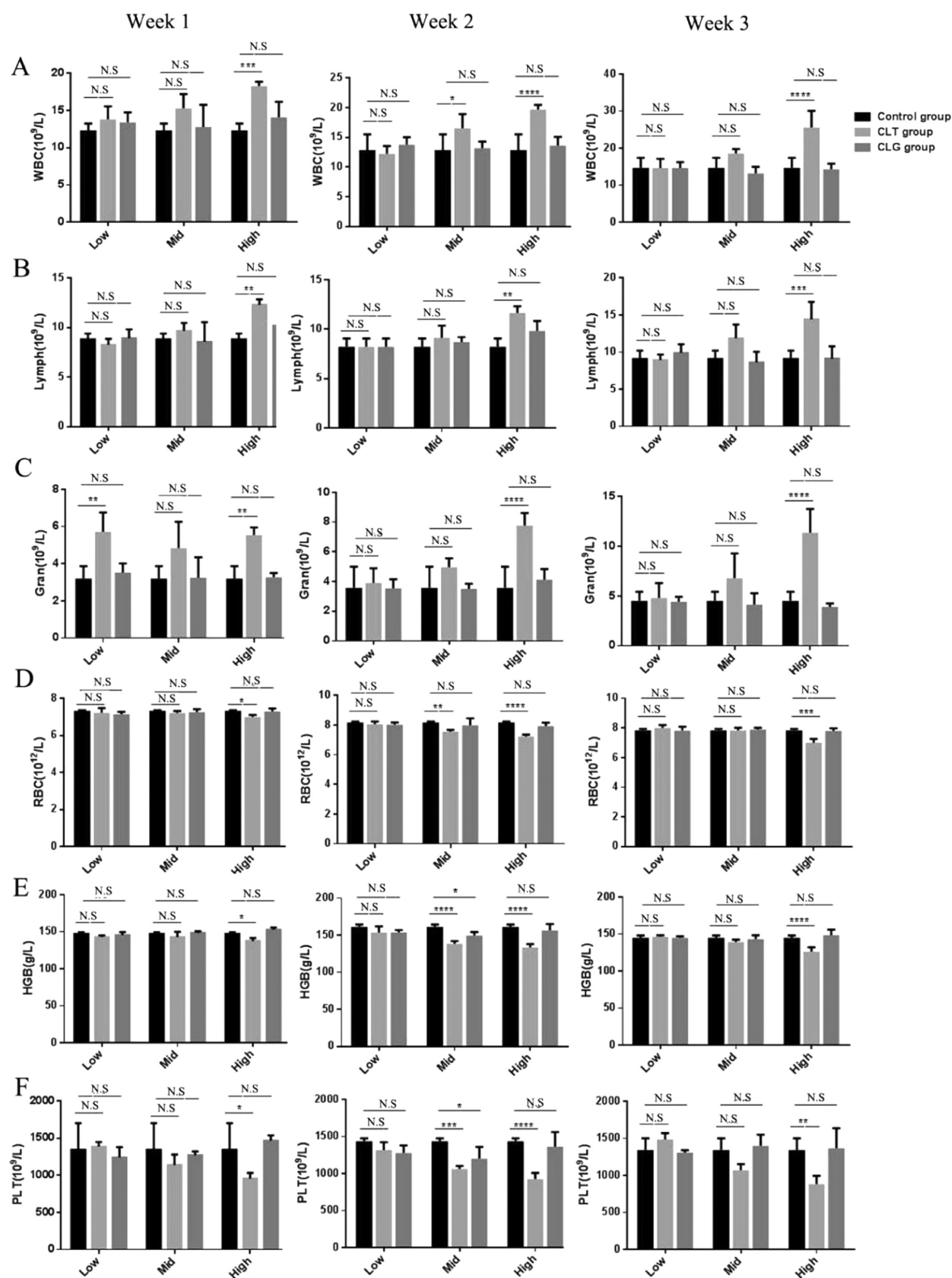


Figure 4. Toxicity of CLT and CLG in blood system. The number of WBC (A) including lymphocyte (B) and granulocyte (C) in rats, which were respectively injected with CLT and CLG, were measured for 3 weeks. The results showed that the high dose (1.8 mg/kg) of CLT significantly contributed to the surge in the leukocyte series cells. The count of red blood cell (RBC) (D), hemoglobin (HGB) (E), and platelet (PLT) (F) were analyzed. RBC and PLT were severely depressed by high dose (1.8 mg/kg) of CLT and almost not influenced by CLG. All of the results are means of measurements from five replicates.

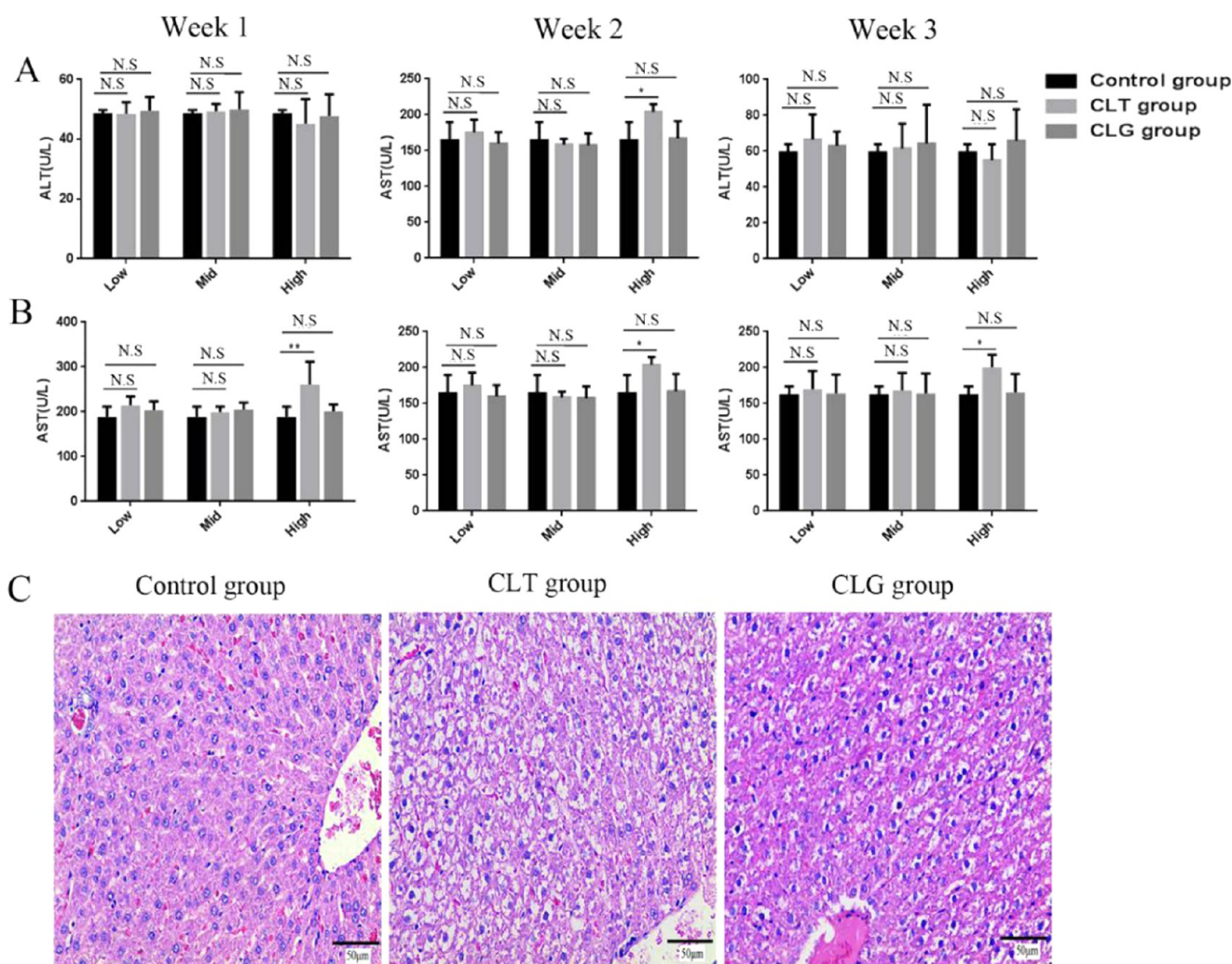


Figure 5. Effect of CLT and CLG on liver in normal rats. The levels of ALT (A) had no alteration and AST (B) reached a high degree when the dose of CLT arrived 1.8 mg/kg. (C) The representative light photomicrographs of H&E stained tissue from the liver. According to the damage score, the control group is marked by (–), the CLT group by (++), and the CLG group by (+). Original magnification in all of the figures was 400X. All of the results are means of measurements from five replicates.

4D), especially at a high dose, which could significantly suppress the number of RBC and cause the downregulation of hemoglobin (HGB) (Figure 4E). In the study, we observed that CLG always performed with consistently stable safety even in the condition of high dose. Taken together, it indicated that CLG also maintained safety to RBC.

Among all of the indexes, the count of blood platelet (PLT) also conducted as a major criterion in the blood system. Apparently, CLT could powerfully restrain the production of PLT, especially when given in the dose of 1.8 mg/kg (Figure 4F). As was predicted, dose gradient of CLG had little influence on the count of PLT, which manifested that the modified compound had the ability to avoid the problem of coagulation dysfunction that CLT always faced. Moreover, what was most interesting was that CLG kept the long-periodic safety even up to 2.62 mg/kg, equaling the dose of CLT of 1.8 mg/kg.

As described above for routine analysis of blood, CLT exactly contributed to surge in the leukocyte series cells, deregulation of RBC, and depression of PLT, especially when the dose reached a high level. However, the newly synthesized derivative, CLG, had little influence on the blood cells, which was certainly up to our expectation.

2.4. No Obvious Harm to Normal Rat Liver in Gradient Dose of CLG. Another factor limiting the use of CLT was that it would partly impair the hepatic cells. As so, we further conducted research on liver indexes, including plasma alanine aminotransferase (ALT), aspartate aminotransferase (AST), and H&E staining.

As was known, AST and ALT are important standards to appraise the extent of damage, so this study consecutively detected the fluctuation of numerical values for 3 weeks. What surprised us was that ALT (Figure 5A) in the CLT-treated groups could keep the concentration as same as that in the control group, but the concentration of AST (Figure 5B) was raised to exceed the average level. According to the results, it demonstrated that CLT was really harmful to hepatic cells, whereas CLG did have little effect, especially when the dose approached the high level.

To further certify the above-mentioned hepatotoxicity, H&E staining was carried out for hepatic damage score. As a result, the liver obtained from the high dose of CLT (1.8 mg/kg) demonstrated obvious characteristics of lesion, including hepatocyte vacuolation, cytoplasm mild swelling, liver sinusitis cell infiltration, and partial liver cell degeneration (Figure 5C).

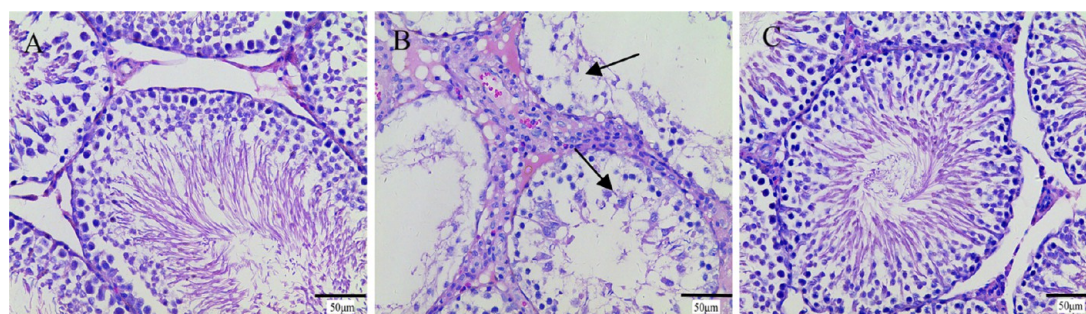


Figure 6. Representative light photomicrographs of H&E-stained tissue from the testis of rats treated with (A) 0.9% saline, (B) CLT (the highest dose of 1.8 mg/kg), and (C) CLG (the highest dose of 2.61 mg/kg). Black arrows indicated areas of damage. According to the damage score, the control group is marked by (–), the CLT group by (+), and the CLG group by (–). The original magnification in all of the figures was 400×. All of the results are means of measurements from five replicates.

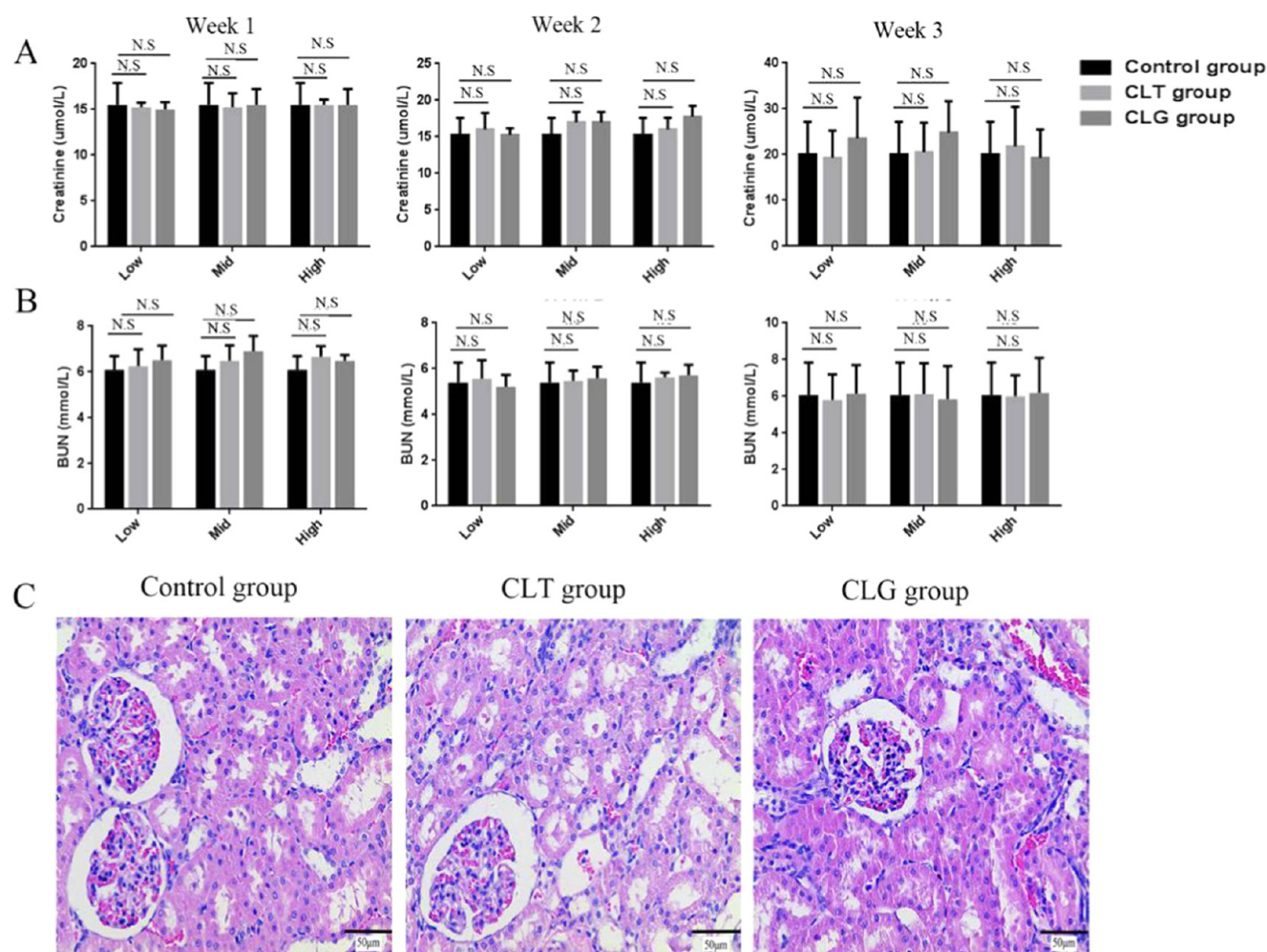


Figure 7. Effect of CLT and CLG on kidney in normal rats. The concentration of plasma (A) Cr and (B) BUN were kept at a steady level, whatever the dose of drugs the rats accepted for 3 weeks. (C) The histological examination showed that CLT (the highest dose of 1.8 mg/kg) and CLG (the highest dose of 2.61 mg/kg) had little influence on the renal tissue. According to the damage score, the control group is marked by (–), the CLT group by (+), and the CLG group by (–). Original magnification in all of the figures was 400×. All of the results are means of measurements from five replicates.

However, the CLG group was really less harmful to the hepatic cells, which maintained a better integrity in texture and function (Figure 5C). These histological alterations almost did not obviously exist in rats injected with CLG. Though the damage score of the CLG group could not totally arrive at the level of the control group, at least, it showed no obvious changes in the histology and morphology compared with the CLT group. The

damage score of CLT and CLG was kept as low as that of the control group, when the injected dose was consistent with the therapeutic dose in renal I/R rats (Figure S5).

CTL did damage liver of the rats; however, the parallel experiment confirmed that CLG could still maintain the hepatic basically healthy.

2.5. No Obvious Toxicity to Productive System of CLG. To our knowledge, CLT was also restricted by reproductive toxicity.²³ Hence, in the present study, we compared the toxic effects of CLG and CLT on rat testis. In the current study, male rat testes collected after 3 week injection were stained with H&E and tested for histologic lesion state. In the CLT groups, especially when the dose reached a high level (Figure 6), evidence showed that the testis tissue had damaged, including varying degrees of denaturation necrosis in convoluted seminiferous tubules, thinning of the epithelium, and absence of spermatozoa in spermatogenic cells. In contrast, the CLG group did not have any focal changes whenever the dose changed from 0.65 to 2.62 mg/kg. From the results, we could basically judge that only when the dose of CLT reached a relative level was the lesion of productive system toxicity obvious. On the contrary, the influence of CLG on the testis tissue was always satisfactory, even up to a high dose. Similarly, the CLG also had no toxicity on the testis of normal rats at doses 0.65 and 1.31 mg/kg (Figure S6). The results of H&E staining examination indicated that CLG induced little toxicity in the male reproductive system, much lower than that caused by CLT when the dose of CLT was changed from 0.45 to 1.8 mg/kg.

2.6. Quite Acceptable Safety of CLG in Kidney, Spleen, Lung, and Heart. In the current study, we also verified that CLG did not harm the kidneys in normal rats. The plasmatic Cr (Figure 7A) and BUN (Figure 7B) were examined, which played an indispensable role in measuring the renal function. The results indicated that the kidneys functioned very well during the administration period of 3 weeks, which properly encouraged it to be full of expectation. Incidentally, we parallelly studied the renal toxicity of CLT. Interestingly, CLT also would not cause alterations in kidney tissue even at the dose of 1.8 mg/kg. To further ensure the safety of CLG and CLT in kidney, the kidney tissues collected 3 weeks after injection were stained with H&E and tested for renal damage degree. Not surprisingly, there was no lesion region in the whole kidney cortex (Figure 7C). The histological examination was totally in accordance with the activity shown by BUN and Cr. Taken together, it demonstrated that compared to CLT itself, the CLT derivative did not bring any toxicity to rat kidneys (Figures 7C and S4).

In addition to kidney, the other organs, such as spleen, lung, and heart, were removed from the rats and stained with H&E for investigating the degree of damage. The H&E images of heart and spleen did not show any obvious damage (Figures S7 and S8). The damage score of lung in the rats injected with CLG was a little lower than that of the group injected with CLT (Figure S9). The CLG-treated group would dysfunction this organ, including the infiltration of the interstitial inflammatory cells, whereas the CLT-treated group did not cause any adverse effect on lung tissue. Though the possibility that CLG would slightly increase the toxicity, which was acceptable, in lung cells, was also confirmed safe, and it could not cover up the main advance in decreasing the CLT toxicity that heavily affected the treatment safety, especially, in the plasma and the urogenital system. Therefore, clinical potential of the novel derivative was promising. It suggested that we might take advantage of both compounds to ameliorate the diseases in the relative organs according to the different conditions.

Taken together, the advance in protective advantages of CLG was much more promising.

3. CONCLUSIONS

Celastrol–glucosamine (CLG) conjugate was first designed and successfully constructed from celastrol (CLT). The CLG could significantly promote the renal recovery for renal I/R injury, similar to CLT, but its toxicity in the blood system, liver, and testis was much slighter than that of CLT. Our results illuminated that CLG would be a great substitute of CLT for the treatment of acute ischemic failure.

4. EXPERIMENTAL SECTION

4.1. Materials. Glucosamine was purchased from Kelong Chemical Reagent Factory (Chengdu, China). CLT (purity of 99.0%) was supplied by Chengdu Must Biotechnology Co. Ltd. (Chengdu, China). Methanol (high-performance liquid chromatography grade) was purchased from Kemiou (Tianjin, China). All of the other chemicals and reagents were of analytical grade obtained commercially.

4.2. Animals. Sprague-Dawley rats (male; body weight: 200 ± 20 g), provided by the West China Experimental Animal Center of Sichuan University (Chengdu, China), were maintained in a special environment and allowed free to food and water. All of the procedures involving animals were approved by the Sichuan University animal ethical experimentation committee, according to the requirements of the National Act on the use of experimental animals (People's Republic of China).

4.3. Synthesis and Characterization of 2-Glucosamine–Celastrol Conjugate. 1-(2-Aminoethoxy)-2-glucosamine was synthesized and certified by our group in previous study,²⁷ and there scarcely existed any isomer in the product. In the current study, we just introduced the detailed synthetic method of CLG (Figure 1). Celastrol (1.11 mmol) and 1-(2-aminoethoxy)-2-glucosamine (4.44 mmol) were dissolved in anhydrous DMF (15 mL) and cooled in ice–water mixture for 30 min. Benzotriazol-1-yl-oxytripyrrolidinophosphonium hexafluorophosphate (0.56 mmol) as a catalyst was dropped slowly into the reacting solution in the condition of stirring, after which, the mixture was allowed to warm up and stirred for another 1 h at room temperature (RT). Then, *N,N*-diisopropylethylamine (0.052 mmol) was added into the mixture drop by drop and stirred for another 40 h until reacting fully. Then, dichloromethane (DCM) (40 mL) was added and the mixture was re-extracted with pure water (20 mL each for 3 times). The aqueous layer was combined and evaporated. The residue was purified with flash chromatography on silica gel giving the pure product as a brownish red powder (mobile phase, DCM/methanol = 12:1). Then, we attempted to investigate whether any diastereoisomer was contained in the product by using a gradient elution in LC-MS, and as expected, the results still maintained a single peak. Moreover, we analyzed the ¹H NMR and ¹³C NMR comprehensively, which could contribute to excluding the possibility of enantiomer.

4.4. Surgical Procedure and Experimental Groups. The renal I/R model was established as described previously.²⁸ Briefly, chloral hydrate (0.35 mg/kg) was intraperitoneally administrated to anesthetize. Then, midline laparotomy was performed and the bilateral renal were subjected to 60 min of ischemia by bilateral renal arteries and veins clamping with no vascular damage followed by reperfusion for 24 h. In the process, when the renal clamps have been removed, the kidneys must be observed for 5 min with the aim to ensure the reflow and then

the incision sutured. After that, the rats were placed in cages, which guaranteed the comfortable environment to recover from anesthesia. Finally, the rats were sacrificed for collecting plasma and kidney specimens (temporarily stored at $-40\text{ }^{\circ}\text{C}$). Blood was obtained from the inferior caval vein and plasma was immediately isolated by centrifugation ($8000g$, 5 min , $4\text{ }^{\circ}\text{C}$).

Before performing a midline laparotomy, male SD rats (body weight of $200 \pm 10\text{ g}$) were randomly assigned into four groups ($n = 5$): (1) sham-operated group, in which the rats were subjected to the same surgical procedure as described but had no induction of renal I/R; (2) I/R group, in which the rats were injected with a vehicle solution via caudal vein 3 days before standard surgical procedure; (3) I/R + CLT group, in which the rats received CLT via caudal vein 3 days before renal ischemia; and (4) I/R + CLG group, in which the rats were injected CLG via caudal vein 3 days before renal ischemia. The vehicle-treated rats received 0.9% saline containing 1% Tween 80 and 10% absolute ethanol.

4.5. Renal Function Parameters for Pharmacological Experiment. Creatinine (Cr) and blood urea nitrogen (BUN) were measured by the assay of serum markers using a chemistry analyzer (Hitachi 7020, Japan), respectively.

4.6. Histological Examination for Pharmacological Experiment. Twenty-four hours after the reperfusion, the rat kidneys were collected and immediately fixed in 4% paraformaldehyde for at least 48 h just at room temperature, dehydrated by grading ethanol and embedded in paraffin. Subsequently, the tissue specimens were cut into $5\text{ }\mu\text{m}$, placed on glass slides, deparaffinized with xylene, hydrated with grading ethanol, and stained with the hematoxylin–eosin (H&E) solution. For the histological evaluation, three kidney sections per rat were examined under a light microscope (Media Cybernetics) at the magnification $100\times$ and $400\times$ by the examiners, respectively. The kidney damage features included tubular dilatation, tubular cell swelling, brush border loss, and cytoplasmic vacuole. The renal injury was semi-quantitatively scored according to the standard described previously: (–) represented normal kidney; (+) minimal damage (less than 5% area of the cortex or outer medulla); (++) mild damage (5–25% area of the cortex or outer medulla); (+++) moderate damage (25–75% involvement of the cortex or outer medulla); and (++++) severe damage (more than 75% involvement of the cortex or outer medulla). Mean scores were presented per group.

Apoptosis of kidney cells was identified by TUNEL assay using In Situ Cell Death Detection Kit (Roche Basel, Switzerland). The paraffin sections of renal tissue ($5\text{ }\mu\text{m}$) were deparaffinized in xylene and rehydrated in a graded ethanol series (100, 90, 80, and 70% for 3 min, respectively). The tissue specimens were dealt with proteinase K for 25 min at room temperature. Then, the sections were stained with preparation of new TUNEL reactive solution, in contrast with positive and negative control groups. Subsequently, $50\text{ }\mu\text{L}$ converter peroxidase was added to the tissue sections for reacting half an hour at room temperature. Finally, $50\text{--}100\text{ }\mu\text{L}$ chromogenic reagent diaminobenzidine (DAB) was dropwise added into staining close to 10 min, observed at $25\text{ }^{\circ}\text{C}$. For appropriate assessment, photomicrographs were taken with a microscope camera (BA400 Digital, Mike audi industrial group Co. Ltd.) at a $100\times$ magnification and $4\times$ magnification, respectively. The percentage of apoptotic cells, apoptotic index, was calculated as the ratio of the number of TUNEL-positive

cells to the total number of cells, calculated in five different random fields.

4.7. Immunohistochemical Staining. Immunohistochemical staining was performed with the Polink-2 Plus Polymer HRP Detection System (Zhongshan Biosciences Inc., China) using the reported protocol. Briefly, paraffin-embedded kidneys were cut at a thickness of $5\text{ }\mu\text{m}$, then deparaffinized and hydrated. The sections were subjected to methanol hydrogen peroxide solution for 10 min at room temperature. Then, the sections were put in 0.01 M citrate buffer (pH 6.0) for incubation at $100\text{ }^{\circ}\text{C}$ for 10 min. Finally, the sections were washed with PBS for 5 min ($2\times$). Subsequently, the sections were incubated with the primary antibodies in phosphate-buffered saline (PBS) against the intercellular adhesion molecule-1, ICAM-1 (1:100; Abcam) and inducible nitric oxide synthase iNOS (1:100; Zhongshan Biosciences Inc.) overnight at $4\text{ }^{\circ}\text{C}$. The sections were washed with PBS for 3 times. Then, the sections were added with diaminobenzidine (DAB) chromogenic agent for reacting 2 min and terminated with running water. The sections were counter-stained with hematoxylin and mounted with resinene. The yellowish-brown signals were considered as positive staining, which was detected under a light microscope (BA400 digital, China) at the magnification of $400\times$.

4.8. Toxicity Assays in Blood and Organs. Rats were randomly divided into seven groups of five animals each. In regard to CLT and CLG, we set a serial dose gradient, in which the sequence dose of CLT was 1.8, 0.9, and 0.45 mg/kg , equaling the sequence of CLG at the dose of 2.62, 1.31, and 0.65 mg/kg . In addition, the control group was injected with the vehicle solution, which consisted of 0.1% Tween-80, 10% absolute ethyl alcohol, and 0.9% saline. All of the groups were administrated 3 times per week for 3 weeks by intravenous injection. All of the rats were weighed every other day to ensure accurate dosing.

During the period of drug delivery, the whole blood was collected by anticoagulated blood-collection tube through the way of orbital blood. Meanwhile, we also collected part of blood in ordinary plastic centrifuge tube and obtained the serum after centrifugation for 8 min by $8000g$. As for the whole blood, it was examined by an automatic biochemical analyzer (Hitachi 7020, Japan), and we could get the information concerning white blood cells (WBCs), red blood cells (RBCs), and platelets (PLTs). As for the serum, it was analyzed for the activity of creatinine (Cr), blood urea nitrogen (BUN), alanine aminotransferase (ALT), and aspartate aminotransferase (AST) using the Hitachi automatic biochemical analyzer.

After 3 weeks, the organs, including heart, liver, spleen, lung, kidney, and testis, were removed and fixed in 4% paraformaldehyde for at least 48 h at room temperature, dehydrated by grading ethanol, and embedded in paraffin. Three sections per rat were counter-stained with H&E and observed under a light microscope (Media Cybernetics) at the magnification $100\times$ and $400\times$. The main aims were to examine whether CLT and CLG could bring alterations to the organs in normal rats.

■ ASSOCIATED CONTENT

📄 Supporting Information

The Supporting Information is available free of charge on the ACS Publications website at DOI: [10.1021/acsomega.7b01890](https://doi.org/10.1021/acsomega.7b01890).

Synthesis of CLG (Section 1); in vitro stability of CLG (Section 2); LC-MS/MS spectrum of CLG (Figure S1); ¹H NMR spectrum of CLG (Figure S2); ¹³C NMR spectrum of CLG (Figure S3); representative light photomicrographs of H&E-stained kidneys of rats (Figure S4); effect of CLT and CLG on the liver in normal rats (Figure S5); representative light photomicrographs of H&E-stained tissue from the testis of rats (Figure S6); representative light photomicrographs of H&E-stained hearts of normal rats (Figure S7); representative light photomicrographs of H&E-stained spleens of normal rats (Figure S8); effect of CLT and CLG on lung in normal rats (Figure S9) (PDF)

AUTHOR INFORMATION

Corresponding Author

*E-mail: qinglin@scu.edu.cn. Tel: 86-28-85501621.

ORCID

Zhirong Zhang: 0000-0001-9118-5394

Qing Lin: 0000-0001-9598-9111

Notes

The authors declare no competing financial interest.

ACKNOWLEDGMENTS

We are grateful for the financial support from the National Science Foundation of China (No. 81690261).

REFERENCES

- (1) Zhang, L.; Wang, F.; Wang, L.; et al. Prevalence of chronic kidney disease in China: a cross-sectional survey. *Lancet* **2012**, *379*, 815–822.
- (2) Choi, K. H.; Kim, S. I.; Shin, S. K.; Moon, J. I.; Kim, Y. S.; Lee, H. Y.; Han, D. S.; Park, K. Renal replacement therapies in the elderly: renal transplantation and continuous ambulatory peritoneal dialysis. *Transplant. Proc.* **2000**, *32*, 333–335.
- (3) Karkouti, K.; Wijeyesundera, D. N.; Yau, T. M.; Callum, J. L.; Cheng, D. C.; Crowther, M.; Dupuis, J. Y.; Fremes, S. E.; Kent, B.; Laflamme, C.; et al. Acute kidney injury after cardiac surgery: focus on modifiable risk factors. *Circulation* **2009**, *119*, 495–502.
- (4) Snoeijs, M. G.; Vink, H.; Voesten, N.; Christiaans, M. H.; Daemen, J.-W. H.; Peppelenbosch, A. G.; Tordoir, J. H.; Peutz-Kootstra, C. J.; Buurman, W. A.; Schurink, G. W. H.; van Heurn, L. W. E. Acute ischemic injury to the renal microvasculature in human kidney transplantation. *Am. J. Physiol.: Renal Physiol.* **2010**, *299*, F1134–F1140.
- (5) Sharfuddin, A. A.; Molitoris, B. A. Pathophysiology of ischemic acute kidney injury. *Nat. Rev. Nephrol.* **2011**, *7*, 189–200.
- (6) Ali, T.; Khan, I.; Simpson, W.; Prescott, G.; Townend, J.; Smith, W.; MacLeod, A. Incidence and outcomes in acute kidney injury: A comprehensive population-based study. *J. Am. Soc. Nephrol.* **2007**, *18*, 1292–1298.
- (7) Snoeijs, M. G. J.; Vaahtera, L.; de Vries, E. E.; Schurink, G. W. H.; Haenen, G. R. M. M.; Peutz-Kootstra, C. J.; Buurman, W. A.; van Heurn, L. W. E.; Parkkinen, J. Addition of a Water-Soluble Propofol Formulation to Preservation Solution in Experimental Kidney Transplantation. *Transplantation* **2011**, *92*, 296–302.
- (8) Hu, L.; Yang, C.; Zhao, T.; Xu, M.; Tang, Q.; Yang, B.; Rong, R.; Zhu, T. Erythropoietin Ameliorates Renal Ischemia and Reperfusion Injury via Inhibiting Tubulointerstitial Inflammation. *J. Surg. Res.* **2012**, *176*, 260–266.
- (9) Esposito, E.; Mondello, S.; Di Paola, R.; Mazzon, E.; Italiano, D.; Paterniti, I.; Mondello, P.; Aloisi, C.; Cuzzocrea, S. Glutamine contributes to ameliorate inflammation after renal ischemia/reperfusion injury in rats. *Naunyn-Schmiedeberg's Arch. Pharmacol.* **2011**, *383*, 493–508.
- (10) Chu, C.; He, W.; Kuang, Y.; Ren, K.; Gou, X. Celastrol protects kidney against ischemia-reperfusion-induced injury in rats. *J. Surg. Res.* **2014**, *186*, 398–407.
- (11) Setty, A. R.; Sigal, L. H. Herbal medications commonly used in the practice of rheumatology: mechanisms of action, efficacy, and side effects. *Semin. Arthritis Rheum.* **2005**, *34*, 773–784.
- (12) Sassa, H.; Kogure, K.; Takaishi, Y.; Terada, H. Structural Basis of Potent Antiperoxidation Activity of the Triterpene Celastrol in Mitochondria - Effect of Negative Membrane-surface Charge on Lipid-oxidation. *Free Radical Biol. Med.* **1994**, *17*, 201–207.
- (13) Huang, F.-C.; Chan, W. K.; Moriarty, K. J.; Zhang, D. C.; Chang, M. N.; He, W.; Yu, K. T.; Zilberstein, A. Novel cytokine release inhibitors. Part I: Triterpenes. *Bioorg. Med. Chem. Lett.* **1998**, *8*, 1883–1886.
- (14) He, W.; Huang, F. C.; Gavai, A.; Chan, W. K.; Amato, G.; Yu, K. T.; Zilberstein, A. Novel cytokine release inhibitors. Part III: Truncated analogs of tripterine. *Bioorg. Med. Chem. Lett.* **1998**, *8*, 3659–3664.
- (15) Jin, H. Z.; Hwang, B. Y.; Kim, H. S.; Lee, J. H.; Kim, Y. H.; Lee, J. J. Antiinflammatory constituents of *Celastrus orbiculatus* inhibit the NF-kappa B activation and NO production. *J. Nat. Prod.* **2002**, *65*, 89–91.
- (16) Westerheide, S. D.; Bosman, J. D.; Mbadugha, B. N. A.; Kawahara, T. L. A.; Matsumoto, G.; Kim, S.; Gu, W.; Devlin, J. P.; Silverman, R. B.; Morimoto, R. I. Celastrols as inducers of the heat shock response and cytoprotection. *J. Biol. Chem.* **2004**, *279*, 56053–56060.
- (17) Fribley, A. M.; Miller, J. R.; Brownell, A. L.; Garshott, D. M.; Zeng, Q.; Reist, T. E.; Narula, N.; Cai, P.; Xi, Y.; Callaghan, M. U.; et al. Celastrol induces unfolded protein response-dependent cell death in head and neck cancer. *Exp. Cell Res.* **2015**, *330*, 412–422.
- (18) Nanjundaiah, S. M.; Venkatesha, S. H.; Yu, H.; Tong, L.; Stains, J. P.; Moudgil, K. D. *Celastrus* and its bioactive celastrol protect against bone damage in autoimmune arthritis by modulating osteoimmune cross-talk. *J. Biol. Chem.* **2012**, *287*, 22216–22226.
- (19) Gu, L.; Bai, W.; Li, S.; Zhang, Y.; Han, Y.; Gu, Y.; Meng, G.; Xie, L.; Wang, J.; Xiao, Y.; et al. Celastrol prevents atherosclerosis via inhibiting LOX-1 and oxidative stress. *PLoS One* **2013**, *8*, No. e65477.
- (20) Kim, D. Y.; Park, J. W.; Jeoung, D.; Ro, J. Y. Celastrol suppresses allergen-induced airway inflammation in a mouse allergic asthma model. *Eur. J. Pharmacol.* **2009**, *612*, 98–105.
- (21) Allison, A. C.; Cacabelos, R.; Lombardi, V. R.; Alvarez, X. A.; Vigo, C. Celastrol, a potent antioxidant and anti-inflammatory drug, as a possible treatment for Alzheimer's disease. *Prog. Neuropsychopharmacology Biol. Psychiatry* **2001**, *25*, 1341–1357.
- (22) Li, Y.; He, D.; Zhang, X.; Liu, Z.; Zhang, X.; Dong, L.; Xing, Y.; Wang, C.; Qiao, H.; Zhu, C.; Chen, Y. Protective effect of celastrol in rat cerebral ischemia model: Down-regulating p-JNK, p-c-Jun and NF-kappa B. *Brain Res.* **2012**, *1464*, 8–13.
- (23) Wang, H. Study on the long term toxicity of celastrol. *Chin. J. Ethnomed. Ethnopharm.* **2017**, *26*, 39–45.
- (24) Yu-Hui, L. I.; Lin, X. Y.; Wang, L. H.; Zhang, S. Y. H.; Yantai. Significance of Mn-SOD, ICAM-1, iNOS in the ischemic preconditioning of rats. *J. Navy Med.* **2011**, *31*, 67.
- (25) Friedewald, J. J.; Rabb, H. Inflammatory cells in ischemic acute renal failure. *Kidney Int.* **2004**, *66*, 486–491.
- (26) Viñas, J. L.; Sola, A.; Genescà, M.; Alfaro, V.; Pí, F.; Hotter, G. NO and NOS isoforms in the development of apoptosis in renal ischemia/reperfusion. *Free Radical Biol. Med.* **2006**, *40*, 992–1003.
- (27) Lin, Y.; Li, Y.; Wang, X.; Gong, T.; Zhang, L.; Sun, X. Targeted drug delivery to renal proximal tubule epithelial cells mediated by 2-glucosamine. *J. Controlled Release* **2013**, *167*, 148–156.
- (28) Chen, G.; Wang, H.; Liu, G.; Chen, W.; He, L.; Sun, S.; Zhang, P. Establishment of an animal model of renal ischemia-reperfusion injury in rats. *J. Fourth Mil.* **2007**, *09*, 812–814.